

Self-assembled nanostructures of specially designed Schiff-bases and their zinc complexes: Preparation, characterization and photoluminescence property

Averi Guha^a, Ria Sanyal^a, Tanmay Chattopadhyay^b, YounGyu Han^c, Tapan Kumar Mondal^d, Debasis Das^{a,*}

^a Department of Chemistry, University of Calcutta, 92, A.P.C. Road, Kolkata 700 009, India

^b Department of Chemistry, Panchakot Mahavidyalya, Sarbari, Neturia, Purulia 723 121, India

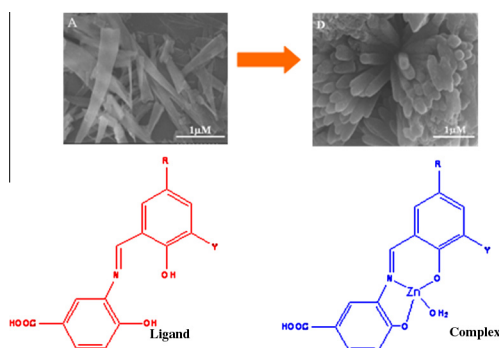
^c Nanotube Research Centre (NTRC), National Institute of Advanced Industrial Science and Technology, Tsukuba Central 5, 1-1-1 Higashi, Tsukuba, Ibaraki 305-8565, Japan

^d Department of Chemistry, Jadavpur University, Jadavpur, Kolkata 700 032, India

HIGHLIGHTS

- Four Schiff-bases and their Zn^{II} complexes has been synthesized with the variation of *para* substituent.
- Inter/intramolecular hydrogen bonding generates self-assembled nanostructures.
- They possess plate, sphere, fiber and granular shape with a size of ~200 nm depending on the R group.
- Powder XRD and FE-SEM was used to characterize their structure.
- DFT calculations were included to rationalize the electronic spectra.

GRAPHICAL ABSTRACT



ARTICLE INFO

Article history:

Received 9 January 2013

Received in revised form 25 March 2013

Accepted 25 March 2013

Available online 2 April 2013

Keywords:

Zn(II)

Schiff-base

SEM

XRD

Fluorescence properties

ABSTRACT

Four specially designed Schiff bases 2-formyl-4-R-6-(3*N*-4-hydroxybenzoic acid)-iminomethyl-phenolato (where R = methyl/*tert*-butyl/chloro for **L1**, **L2**, **L3** respectively) and 2-(3*N*-4-hydroxybenzoic acid)-iminomethyl-phenolato (**L4**) having ability to form hydrogen bonding and their zinc complexes (**1–4**) have been synthesized and characterized. These complexes gave various types of nano-sized materials via self-assembly in solid state. FE-SEM was employed to investigate their morphology. Using a variety of analytical techniques such as elemental analysis, infrared spectroscopy (FT-IR), ESI-MS and ¹H NMR spectroscopy, a consistent picture of structures of these complexes are obtained. All the Schiff-bases and their zinc complexes exhibit photoluminescence property. Density functional theory calculation has been performed to rationalize the origin of the spectral bands of the ligands as well as the complexes.

© 2013 Published by Elsevier B.V.

1. Introduction

Nanoscience and nanotechnology are genuinely promising to the extent that they have significant potential to have a remarkable impact on our society. Generating nanoparticles from

* Corresponding author. Tel.: +91 33 24837031; fax: +91 33 23519755.

E-mail address: dasdebasis2001@yahoo.com (D. Das).

functionally defined precursors encompasses a magnificent research area due to the fundamental interest of mankind in materials that have practical applications in chemistry, biology, physics, and related interdisciplinary fields. Well-structured deliberate architectures on surface with particular emphasis on supramolecular self-assembly provide attractive features in this regard. It is essentially a 'bottom-up' approach which allows the simple and rapid formation of designed functional surface

assemblies [1,2]. These can be brilliantly tuned through the optimal choice of molecular building blocks utilized and stabilized by hydrogen bonding [3–8], van der Waals interactions [9], π - π bonding [10,11] or metal coordination [12,13] between the blocks. This comprises the most important and handy techniques for the spontaneous construction of nanostructures such as particle, fiber, and layer [14,15]. Among them self-assembled entities generated via hydrogen bonding is the most popular. The choice of molecular shape and size and especially the arrangement of hydrogen-bonding donor and acceptor sites are crucial to generate unique supramolecular nanostructures. Hydrogen bonding is not random but selective and controlled by the directional strength of intermolecular interactions [16]. Hydrogen bonds are formed when a donor (D) with an available acidic hydrogen atom is brought into direct contact with an acceptor (A). It is the central theme to regulate the spatial arrangement of functionalized molecules and ions in the solid state and on surfaces [17–20]. Nevertheless one of the biggest challenges of supramolecular chemistry till date is earlier evaluation of molecular systems that would lead to preprogrammed perfectly controlled self-assembly [21]. We know that carboxylic acids can form hydrogen-bonding patterns that contain a center of symmetry, the *dimer motif*, and also aggregate in centric one-dimensional chains, *catamers*, resulting from the formation of hydrogen bonds to two or more neighboring building blocks. They are conventional motif-controlling functional elements in the field of crystal engineering as well as supramolecular self-assembly [22]. For the development of coordination chemistry, Schiff bases have been widely studied due to their straightforward synthetic pathways. Moreover their complexes have biological resemblance and excellent catalytic activity in versatile chemical reactions [23]. They can easily serve as the N, O or S-donor ligands. The nature, quantity and relative position of donor atoms and metal centers play an important role for the construction of controlled supramolecular self-assembled structures [24]. The motivation to study the specially designed Schiff bases as guest is due to the fact that they are molecules with a potential to form intermolecular hydrogen bond and also to investigate the effect of different *para* substituent on morphology. Further, metal complexation allows the formation of more rigid architectures and because of the different complexation modes, this kind of interaction can be used for the formation of templates, which are the basis for extension from the second to the third dimension. We have investigated the self-assembly, if any, of newly synthesized Schiff bases (**L1–L4**) and their zinc complexes (**1–4**) as depicted in Scheme 1 and attempted to rationalize them.

2. Experimental

2.1. Materials

All chemicals were obtained from commercial sources and used as received. Solvent and reagents were purified and dried according to standard procedures [25]. All other reagents were used as obtained from either Aldrich or Fluka.

2.2. Methods and instrumentation

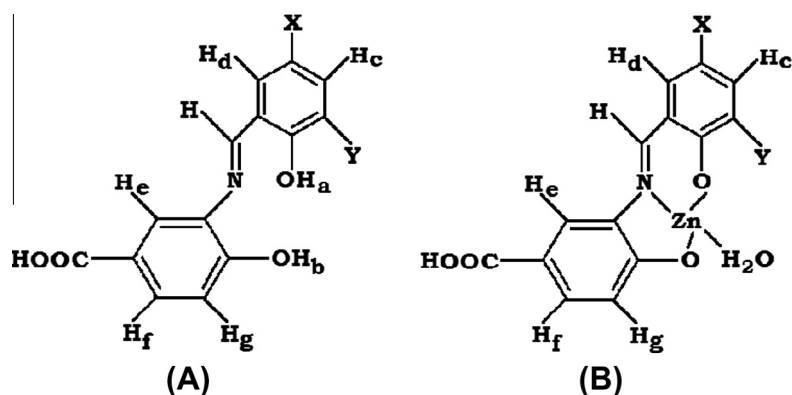
Reactions were monitored by TLC on silica gel plates (Machery-Nagel POLYGRAM SIL G/UV254). Visualization of the spots were carried out by fluorescence quenching with UV light at 254 nm. The NMR spectra for standard characterization purposes were recorded at room temperature with a Bruker AV300 Supercon NMR spectrometer using the solvent signal as the internal standard in a 5 mm BBO probe. The ^1H NMR spectra were recorded at 300 MHz. The chemical shifts are relative to the signals of the used solvents: DMSO in DMSO- d_6 ($\delta_{\text{1H}} = 2.50$) [26]. The apparent coupling constants are given in Hertz. The description of the fine structure means: s = singlet, br.s = broad signal, d = doublet, t = triplet and sb = singlet with broken heads. Elemental analyses (carbon, hydrogen, and nitrogen) were performed using a PerkinElmer 24 °C elemental analyzer. Infrared spectra ($4000\text{--}400\text{ cm}^{-1}$) were recorded at 27 °C using a Shimadzu FTIR-8400S where KBr was used as medium. Electronic spectra (800–200 nm) were obtained at 27 °C using a Shimadzu UV-3101PC where DMSO was used as a medium as well as a reference. Fluorescence spectra of the complexes in DMSO were recorded in a Perkin-Elmer model LS 55 Luminescence spectrometer. The electrospray mass spectra were recorded on a MICROMASS Q-TOF mass spectrometer.

2.3. Syntheses of complexes

2.3.1. Ligand 1 – L1

The Schiff-base was prepared by condensation reaction between an aldehyde and a primary amine. An ethanolic solution (10 mL) of 3-amino-4-hydroxy benzoic acid (10 mmol) was added dropwise to an ethanolic solution (15 mL) of 2,6-diformyl-4-methyl-phenol (10 mmol) with constant stirring. The resultant mixture was refluxed for 6 h and the solvent was reduced by rotary evaporator. The solid mass thus obtained was recrystallised several times from dry ethanol to get the pure ligand.

Yield: 69%. Anal. Calcd. for $\text{C}_{16}\text{H}_{13}\text{NO}_5$: C, 64.21; H, 4.37; N, 4.66. Found: C, 63.28; H, 4.32; N, 4.62%.



Scheme 1. (A) Ligands: **L1**: X = $-\text{CH}_3$, Y = $-\text{CHO}$; **L2**: X = $-\text{C}(\text{CH}_3)_3$, Y = $-\text{CHO}$; **L3**: X = $-\text{Cl}$, Y = $-\text{CHO}$; **L4**: X = Y = $-\text{H}$. (B) Complexes: **1**: X = $-\text{CH}_3$, Y = $-\text{CHO}$; **2**: X = $-\text{C}(\text{CH}_3)_3$, Y = $-\text{CHO}$; **3**: X = $-\text{Cl}$, Y = $-\text{CHO}$; **4**: X = Y = $-\text{H}$.

^1H NMR (300 MHz, DMSO- d_6 , 25 °C) δ = 15.107 (s, 1H, COOH), 14.728 (br, 1H, OH_a), 10.395 (s, 1H, CHO), 10.293 (br, 1H, OH_b), 9.142 (s, 1H, N=CH), 7.894 (s, 1H, H_c), 7.803, 7.809 (sb, H_e), 7.768 (s, 1H, H_d), 7.687, 7.680 (d, 1H, H_f), 7.018, 7.000 (d, 1H, H_g), δ 2.221 (s, 3H, CH₃).

FT-IR ν (KBr) [cm^{-1}] = 1683(s), 1634(s), 1598(s), 1462(s).

ESI-MS m/z = 300.2496 (calculated for $^{12}\text{C}_{16}\text{H}_{13}\text{NO}_5 + \text{H}^+$: 300.2859).

2.3.2. Ligand 2 – L2

It was prepared by adopting similar procedure as for L1 where the aldehyde used was 2,6-diformyl-4-*tert*-butyl-phenol instead of 2,6-diformyl-4-methyl-phenol.

Yield: 72%. Anal. Calcd. for C₁₉H₁₉NO₅: C, 66.85; H, 5.61; N, 4.10. Found: C, 66.83; H, 5.60; N, 4.08%.

^1H NMR (300 MHz, DMSO- d_6 , 25 °C) δ = 15.109 (s, 1H, COOH), 14.734 (br, 1H, OH_a), 10.389 (s, 1H, CHO), 10.287 (br, 1H, OH_b), 9.026 (s, 1H, NH), 7.968 (s, 1H, H_c), 7.812, 7.809 (sb, 1H, H_e), 7.768 (s, 1H, H_d), 7.674, 7.650 (d, 1H, H_f), 6.987, 6.965 (d, 1H, H_g), 1.152 (s, 9H, C(CH₃)₃).

FT IR ν (KBr) [cm^{-1}] = 1685(s), 1623(s), 1516(s), 1460(s).

ESI-MS m/z = 342.3321 (calculated for $^{12}\text{C}_{19}\text{H}_{19}\text{NO}_5 + \text{H}^+$: 342.3659).

2.3.3. Ligand 3 – L3

The same procedure as for L1 was repeated by using 2,6-diformyl-4-chloro-phenol as the aldehyde.

Yield: 70%. Anal. Calcd. for C₁₅H₁₀NO₅Cl: C, 56.35; H, 3.15; N, 4.36. Found: C, 56.31; H, 3.12; N, 4.34%.

^1H NMR (300 MHz, DMSO- d_6 , 25 °C) δ = 15.105 (s, 1H, COOH), 14.730 (br, 1H, OH_a), 10.392 (s, 1H, CHO), 10.285 (br, 1H, OH_b), 9.049 (s, 1H, NH), 7.995 (s, 1H, H_c), 7.806, 7.804 (sb, H_e), 7.767 (s, 1H, H_d), 7.561, 7.558 (d, H_f), 7.018, 7.001 (d, H_g).

FT IR ν (KBr) [cm^{-1}] = 1680(s), 1629(s), 1528(s), 1384(s).

ESI-MS m/z = 320.7762 (calculated for $^{12}\text{C}_{15}\text{H}_{10}\text{NO}_5\text{Cl} + \text{H}^+$: 320.7049).

2.3.4. Ligand 4 – L4

The same synthetic strategy was used as for L1 where salicylaldehyde was used instead of 2,6-diformyl-4-methyl-phenol.

Yield: 65%. Anal. Calcd. for C₁₄H₁₁NO₄: C, 65.37; H, 4.31; N, 5.44. Found: C, 65.35; H, 4.30; N, 5.42%.

^1H NMR (300 MHz, DMSO- d_6 , 25 °C) δ = 13.598 (s, 1H, COOH), 10.762 (br, 1H, OH_a), 10.659 (br, 1H, OH_b), 9.088 (s, 1H, NH) and the peaks between δ 7.959 and δ 6.718 correspond to the aromatic hydrogens of the two benzene rings.

FT IR ν (KBr) [cm^{-1}] = 1690(s), 1513(s), 1380(s).

ESI-MS m/z = 280.2679 (calculated for $^{12}\text{C}_{14}\text{H}_{11}\text{NO}_4 + \text{Na}^+$: 280.2308).

2.3.5. Complex 1

A methanolic solution (10 mL) of zinc(II) acetate hydrate (5 mmol) was added dropwise to a methanolic solution (10 mL) of pure Schiff-base ligand L1 (5 mmol) with constant stirring. The complex began to precipitate out immediately after the completion of addition of ligand. The stirring was continued for another 2 h, filtered and kept in a CaCl₂ desiccator.

Yield: 68%. Anal. Calcd. for C₁₆H₁₃NO₆Zn: C, 50.48; H, 3.44; N, 3.68. Found: C, 50.43; H, 3.40; N, 3.65%.

^1H NMR (300 MHz, DMSO- d_6 , 25 °C) δ = 15.15 (s, 1H, COOH), 10.500 (s, 1H, CHO), 9.091 (s, 1H, N=CH), 7.891 (s, 1H, H_c), 7.811, 7.817 (sb, H_e), 7.768 (s, 1H, H_d), 7.687, 7.680 (d, 1H, H_f), 6.898, 6.801 (d, 1H, H_g), δ 2.355 (s, 3H, CH₃).

FT IR ν (KBr) [cm^{-1}] = 1717(s), 1634(s), 1534(s), 1354(s).

ESI-MS m/z = 403.6750 (calculated for $^{12}\text{C}_{16}\text{H}_{13}\text{NO}_6\text{Zn} + \text{Na}^+$: 403.6468).

2.3.6. Complex 2

It was prepared by the same process as above where the Schiff-base ligand used was L2 instead of L1.

Yield: 68%. Anal. Calcd. for C₁₉H₁₉NO₆Zn: C, 53.98; H, 4.53; N, 3.31. Found: C, 53.93; H, 4.51; N, 3.30%.

^1H NMR (300 MHz, DMSO- d_6 , 25 °C) δ = 14.964 (s, 1H, COOH), 10.279 (s, 1H, CHO), 9.120 (s, 1H, N=CH), 7.972 (s, 1H, H_c), 7.812, 7.813 (sb, 1H, H_e), 7.770 (s, 1H, H_d), 7.675, 7.654 (d, 1H, H_f), 7.003, 6.971 (d, 1H, H_g), 1.144 (s, 9H, C(CH₃)₃).

FT IR ν (KBr) [cm^{-1}] = 1700(s), 1630(s), 1594(s), 1383(s).

ESI-MS m/z = 423.7793 (calculated for $^{12}\text{C}_{19}\text{H}_{19}\text{NO}_6\text{Zn} + \text{H}^+$: 423.7449).

2.3.7. Complex 3

The same method was repeated where ligand L3 was used instead of L1.

Yield: 68%. Anal. Calcd. for C₁₅H₁₀NO₆ClZn: C, 44.92; H, 2.51; N, 3.49. Found: C, 44.90; H, 2.48; N, 3.47%.

^1H NMR (300 MHz, DMSO- d_6 , 25 °C) δ = 15.233 (s, 1H, COOH), 10.108 (s, 1H, CHO), 9.341 (s, 1H, N=CH), 7.910 (s, 1H, H_c), 7.806, 7.804 (sb, H_e), 7.767 (s, 1H, H_d), 7.561, 7.558 (d, H_f), 7.154, 7.069 (d, H_g).

FT IR ν (KBr) [cm^{-1}] = 1717(s), 1634(s), 1534(s), 1365(s).

ESI-MS m/z = 424.0319 (calculated for $^{12}\text{C}_{15}\text{H}_{10}\text{NO}_6\text{ClZn} + \text{Na}^+$: 424.0658).

2.3.8. Complex 4

A similar synthetic strategy was employed as for other complexes where ligand L4 was used instead of L1.

Yield: 68%. Anal. Calcd. for C₁₄H₁₁NO₅Zn: C, 49.66; H, 3.27; N, 4.41. Found: C, 49.63; H, 3.25; N, 4.38%.

^1H NMR (300 MHz, DMSO- d_6 , 25 °C) δ = 13.804 (s, 1H, COOH), 9.052(s, 1H, N=CH) and the peaks between δ 7.959 to δ 6.718 correspond to the aromatic hydrogens of the two benzene rings.

FT IR ν (KBr) [cm^{-1}] = 1695(s), 1556(s), 1338(s).

ESI-MS m/z = 361.6230 (calculated for $^{12}\text{C}_{14}\text{H}_{11}\text{NO}_5\text{Zn} + \text{Na}^+$: 361.6108).

2.4. Electron microscopic observation

Field-emission scanning electron microscope (FE-SEM) images were taken using a Hitachi S-4800 field emission electron microscope at 15 kV. Specimens were prepared by placing a 3 μL drop of the dispersion on an amorphous carbon supporting film mounted on a standard grid. The drop was then blotted off with a filter paper, followed by evaporation to dryness in vacuo. These dried samples on the grids were coated with 2–3 nm thickness of osmium using a Meiwaforsis Neoc AN.

2.5. Spectroscopic analyses

FT-IR spectra were obtained on a Shimadzu FTIR-8400S spectrometer using KBr method. X-ray diffraction (XRD) was performed on a Rigaku R-AXIS IV X-ray diffractometer monochromated Cu K α radiation (40.0 kV, 30.0 mA) at room temperature.

2.6. Computational methods

Full geometry optimizations were carried out using the density functional theory method at the B3LYP level for ligands L1–L4 and the complex 1–4 [27]. All elements except Zn were assigned the 6-31+G(d) basis set. The LANL2DZ basis set with effective core potential was employed for the Zn atom [28]. The vibrational frequency calculation was performed to ensure that the optimized geometries represent the local minima and there are only positive eigen values. All calculations were performed with Gaussian03 program

package [29] with the aid of the GaussView visualization program. Vertical electronic excitations based on B3LYP optimized geometries were computed using the time-dependent density functional theory (TD-DFT) formalism [30] in DMSO using conductor-like polarizable continuum model (CPCM) [31].

3. Results and discussion

3.1. Synthesis and characterization

All the Schiff-base ligands (**L1–L4**) were prepared by following the same condensation procedure (see SI file). The compounds with carboxylate functional group can be conveniently characterized by IR spectroscopy. Generally, the peak at wave numbers around 1680–1700 cm^{-1} , which is assignable to the C=O stretching vibration, indicate a hydrogen bonding mode between the COOH groups. The peak in the range of 1680–1690 cm^{-1} indicates the existence of an acid–acid dimer, whereas the peak at 1700 cm^{-1} and above indicates a lateral-type hydrogen-bond [32–36]. We have carried out FT-IR measurements of all Schiff bases (**L1–L4**) and their zinc complexes (**1–4**). The characteristic IR band frequencies are summarized in Table 1.

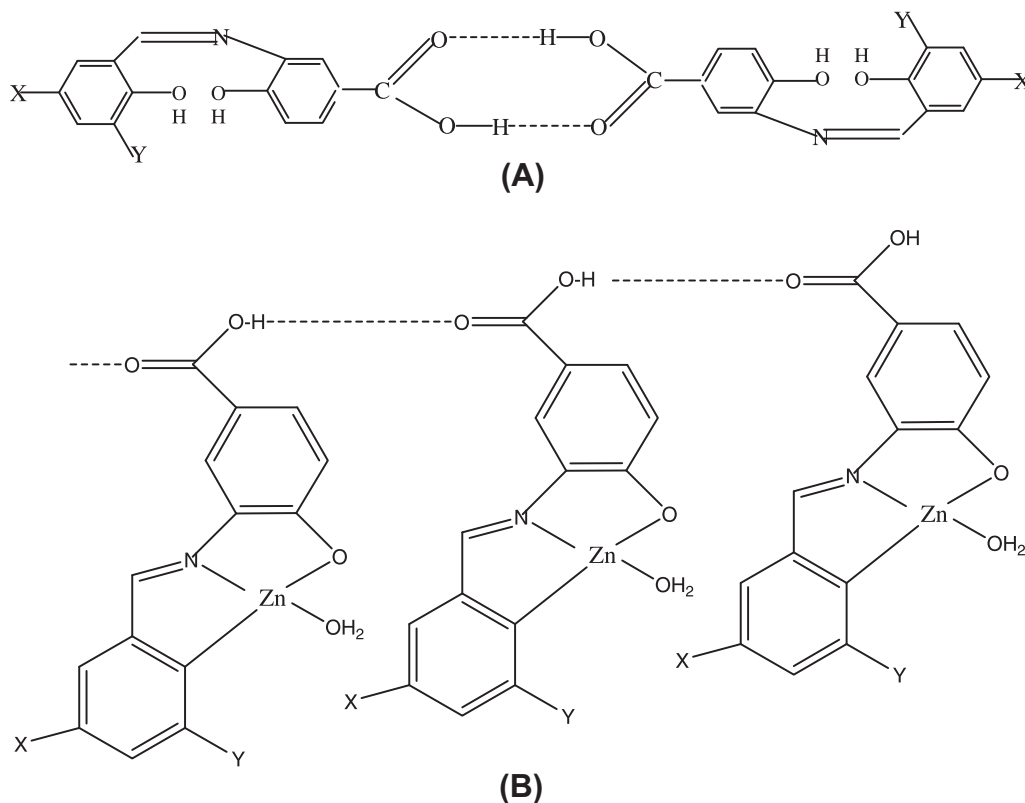
All the ligands have a peak in the range 1680–1690 cm^{-1} for the stretching frequency of the carbonyl group of –COOH group. On the other hand, the zinc complexes exhibit a peak in the range

1700–1720 cm^{-1} which is assigned for –COOH group. Thus it is evident that that the (SI Figs. 1–8 in Supporting information) –COOH group do not participate in complex formation, but they form lateral-type hydrogen-bond which assists in the formation of nanostructures via self assembly (Scheme 2). In addition, there are bands in the range 3000–3400 cm^{-1} , 2200–2800 cm^{-1} and at $\sim 1630 \text{ cm}^{-1}$ for phenolic –OH groups, –C–H skeletal vibration and –CHO groups respectively.

The ligands were further characterized by ^1H NMR spectroscopy (see SI Figs. 9–12 in Supporting information), where for **L1**, **L2** and **L3** (Scheme 1) a singlet signal at $\delta \approx 15.1$ corresponds to the hydrogen of carboxylic acid group, the broad peaks at $\delta \approx 14.7$ and 10.3 stands for phenolic OH_a and OH_b respectively, the aldehyde hydrogen arises at $\delta \approx 10.4$ and that for the imine hydrogen at 9.1. The peaks in between $\delta 7.0$ to $\delta 8.0$ correspond to the aromatic hydrogens of the two benzene rings present in the ligand system where H_c and H_d appear as singlet at $\delta \approx 7.9$ and 7.8 respectively but metacoupled H_e give singlet with broken heads at $\delta \approx 7.803$, 7.809. The peaks at $\delta \approx 7.687$, 7.680 are for H_f which is orthocoupled with H_g and with broken heads for metacoupled with H_e , doublet at $\delta \approx 7.018$, 7.000 are for H_g which doublet orthocoupled with H_f . The three hydrogens of the methyl group for **L1** appear as a singlet at $\delta 2.3$ nine tert-butyl hydrogens at $\delta 1.3$ for **L2**. For the **L4** the bands show a slight shifting with respect to the others at $\delta \approx 13.6$ for carboxylic acid group, 10.8, 10.7 (each for the two hydrogens of OH_a and OH_b), 9.1 for imine hydrogen.

Table 1
Infrared spectral data in cm^{-1} .

Functional groups	L1	L2	L3	L4	1	2	3	4
COOH group	1683	1685	1680	1690	1717	1700	1717	1695
CHO group	1634	1623	1629	–	1634	1630	1634	–
Imine group	1598	1516	1528	1513	1534	1594	1534	1556
Skeletal vib.	1462	1460	1384	1380	1354	1383	1365	1338



Scheme 2. Two different types of hydrogen-bonding modes between the COOH groups displaying (A) acid–acid dimer (B) lateral type hydrogen bonding.

The complexes (**1–4**) were also characterized by proton NMR (see SI Figs. 31–34 in Supporting information) where each spectrum resembles that of the corresponding ligand except the fact that the phenolic OH groups which gets deprotonated during complexation have vanished.

3.2. Scanning electron microscopy studies and powder X-ray diffraction

Field-emission scanning electron microscopy (FE-SEM) was used to analyze the self-assembled nanostructure of the resulting compounds (Fig. 1). The morphologies of the Schiff-base ligands

(**L1**, **L2**, **L3** and **L4**) were observed to be different depending on the ligand group at *para*-position, i.e., $-\text{CH}_3$, $-\text{C}(\text{CH}_3)_3$, $-\text{Cl}$ and $-\text{H}$. The ligand **L1** showed sheet shape of $\sim 2 \mu\text{m}$ length and $\sim 200 \text{ nm}$ diameter (Fig. 1A). The ligand **L2** illustrated spherical particles of size $\sim 100 \text{ nm}$ (**1C**). The ligand **L3** exhibited amorphous agglomerates of size $\sim 200 \text{ nm}$ (**1E**). The ligand **L4** showed granular shape with the size of $\sim 250 \text{ nm}$ (**1G**). We observed significant change in the ligands morphology when zinc ion was added to them (i.e. in the complex). The complexes, **1** and **4**, both showed fiber like shape (Fig. 1B and H), but their size was quite different. The complex **1** have $\sim 1 \mu\text{m}$ length and $\sim 100 \text{ nm}$ diameter whereas complex **4** have $\sim 1 \mu\text{m}$ length and $\sim 50 \text{ nm}$ diameter. In case of the

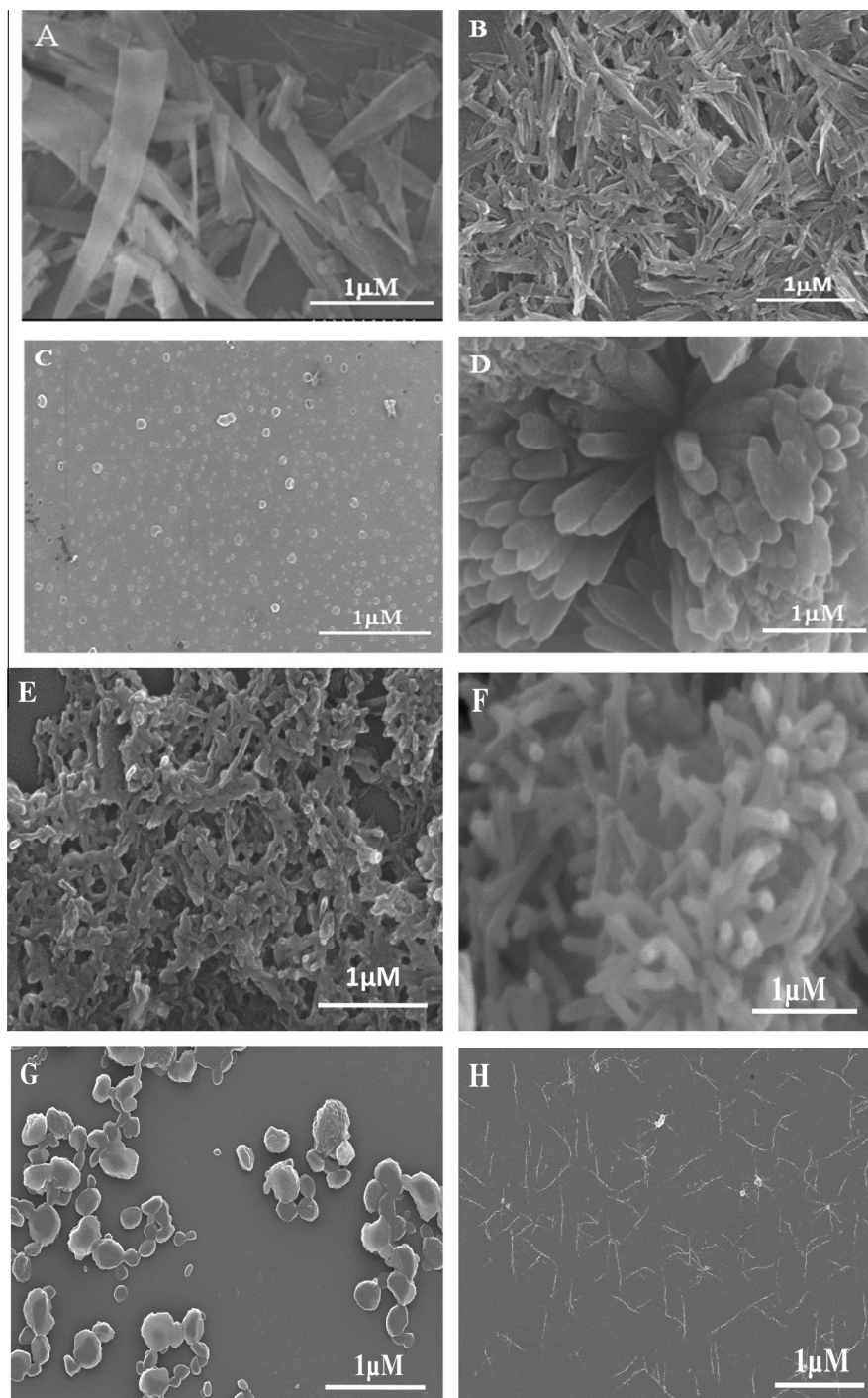


Fig. 1. FE-SEM images of the designed Schiff-bases (A: **L1**, C: **L2**, E: **L3** and G: **L4**) and their zinc complexes (B: **1**, D: **2**, F: **3**, H: **4**).

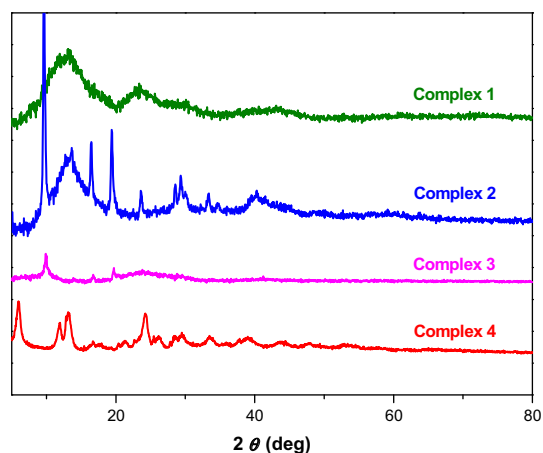


Fig. 2. XRD pattern of the zinc complexes: a = 1; b = 2; c = 3; d = 4.

complexes **2** and **3**, both have same rod shape (Fig. 1D and F) with a size of $\sim 1 \mu\text{M}$ length and $\sim 200 \text{ nm}$ diameter.

This change in morphology of the various ligands indicates that the morphology of supramolecular aggregation can be controlled by introducing groups of various steric properties. The methanolic mixture of Zinc(II) acetate and Schiff-bases forms a precipitate each time we had attempted for crystallization. Just for the aim to investigate the inherent physical nature of the complexes, powder XRD of the complexes were carried out. Fig. 2 shows the XRD for the precipitated samples. It reveals that all the complexes are crystalline solids to some degree. Complex **2** and **4** appears to be the most crystalline in the set followed by complex **1** and then **3** which can be considered to be almost amorphous. It is probably again the substitution at *para* position which governs the crystallinity of the samples and hence their XRD patterns.

Thus it can be suggested that the bulky ligands have a tendency to form a crystalline structure although it is difficult to describe the detailed molecular packing structures from the patterns. **2** and **3** have similar crystal peaks at 9.1° , 16.4° , and 19.4° . It gives support to the fact that they form similar inter and intramolecular hydrogen bonds in the complexes and their rod like shape in Fig. 1B and C is supposed to result from these interactions. The diffraction of **4** shows a sharp peak at 6° , which is mainly attributed to the formation of imine groups and the cleavage of intra-molecular hydrogen bond [37]. Notably, the change in crystalline nature is mainly dependant on some factors induced by a ligand, such as steric hindrance and hydrophobic force [38]. Thus, it is likely that the crystalline nature can be regulated by the modification of substituent groups in Schiff-bases.

3.3. Absorption and fluorescence properties

All the designed Schiff-bases exhibit three absorption bands while their zinc complexes show two peaks which are summarized in Table 2. The absorption spectra of **L1** have been recorded in DMSO solvent and presented in Fig. 3a. **L1** is found to exhibit three absorption bands peaking at $\lambda_{\text{abs}} \approx 267 \text{ nm}$, 316 nm and 467 nm .

Usually it is difficult to perturb the spectral properties of Schiff-bases by external agents (like change of solvent polarity, pH, etc.)

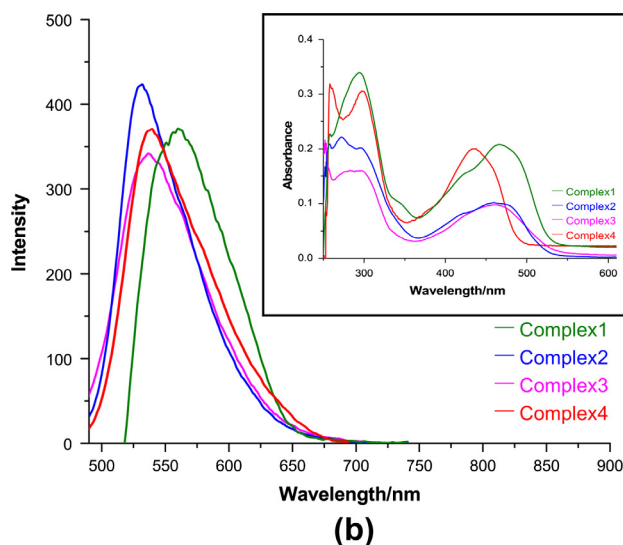
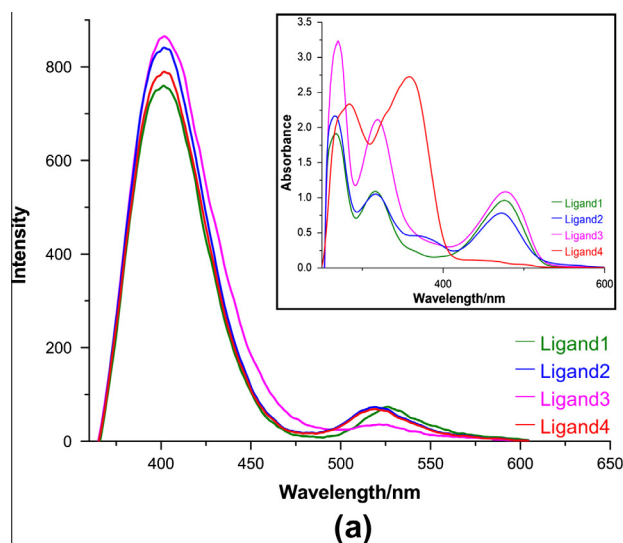


Fig. 3. The absorption (inset) and emission spectra of the (A) Schiff bases (B) their zinc complexes in DMSO at a concentration of 10^{-4} M at room temperature.

so that an unequivocal assignment for the spectral properties of Schiff-bases is often laid aside [30–32]. In our case too we have faced similar difficulties. Moreover, solubility of the compounds in other solvents were quite poor making spectral characterization further difficult. However, with a view to the fact that **L1** contains a substituted benzaldehyde type chromophore the absorption bands at $\approx 267 \text{ nm}$ and $\approx 367 \text{ nm}$ seems to be originating from the open form and intramolecularly hydrogen bonded closed form of **L1**, respectively. It is probably the greater degree of stability due to the presence of the intramolecular hydrogen bonding (IMHB) interaction that the closed form absorbs at lower energy region ($\lambda_{\text{abs}} \approx 367 \text{ nm}$). Though the assignment of the lowest energy absorption band ($\lambda_{\text{abs}} \approx 467 \text{ nm}$) remains a matter of debate, a direct comparison with spectroscopic properties of structurally related compounds

Table 2
Electronic and photoluminescence spectral data in nm.

	L1	1	L2	2	L3	3	L4	4
Absorption	267, 316, 467	292, 466	266, 316, 472	296, 461	267, 319, 475	298, 457	285, 349, 468	300, 436
Emission	404, 401, 529 527	402, 558	404, 401, 521 520	403, 533	406, 399, 522 523	407, 538	405, 404, 525 524	408 530

[39–41] tends to attribute the band to the zwitterionic species. Also this observation seems to be self-authenticated by the fact that the zwitterionic species is capable of undergoing substantial stabilization through delocalization of its formal charges whence it absorbs in the lower energy region.

To understand the spectral bands specially the low energy transitions of the ligands, TD-DFT calculations on the optimized geometries of **L1–L4** are performed in DMSO solvent. The low energy bands are only found in the zwitterionic forms of the ligands. Other calculated spectral transitions also well reproduced the experimental bands with this form of the ligands (Fig. 4 and see SI Figs. 21–28 in Supporting information). To study the effect of Zn²⁺ ion on the spectral properties of the ligands, the respective Zn(II) complexes in penta-coordinated geometries (two coordination site have been occupied by MeOH as is assigned by ESI-MS study from the spectra given in SI Figs. 13–20 in Supporting information) have been optimized and TD-DFT calculations were performed. The optimized structures of the ligands and complexes are given in SI Figs. 29 and 30 in Supporting information. There are no significant change in the spectral bands of the complexes compared to free ligand values except the blue-shifting of the low energy bands (see SI Tables 1–8 in Supporting information).

The emission spectra of **L1** recorded at $\lambda_{ex} \approx 316$ nm and 467 nm are presented in Fig. 3a. It is usual to observe that excitation at the respective species produces the corresponding local emission maxima at $\lambda_{em} \approx 400$ nm and 528 nm. However, for $\lambda_{ex} \approx 316$ nm a little hump at $\lambda_{em} \approx 528$ nm is observed corresponding to the local emission from the zwitterionic species.

It is not unlikely that electronic excitation at the higher energy excitation wavelength of 316 nm may lead to formation of the zwitterionic species on the excited state surface to some extent. The emission spectra of the four Zn^{II} complexes are depicted in Fig. 3b and inset show the absorption spectra of those species. The complexation with Zn²⁺ ion is not found to perturb the spectral properties of **L1** significantly except for a red-shift on the emission profile to $\lambda_{em} \approx 558$ nm with accompanied lowering of intensity. We have observed similar results for the other ligands (**L2–L4**) and their zinc complexes (**2–4**).

4. Conclusion

We have begun by synthesizing various self-assembled nano-sized materials from four Schiff-bases and their zinc complexes

in high yield by a simple synthetic approach. The Schiff-bases have been designed in such a way that they may form inter and/or intra molecular hydrogen bonding, a property which has been proved to be instrumental in making self-assembled materials. The morphology of the Schiff-base ligands are observed to be markedly influenced by the substituent groups present in the backbone of the ligand systems. Also, for a particular ligand the morphology gets changed on complexation with Zn(II) ion. The crystalline nature of the complexes differs on varying the substituent on the ligand backbone. Thus, the present study demonstrates the tuning possibilities of supramolecular arrays giving an insight into the new strategies for fabricating nanostructural architectures. The synthesized compounds also have pronounced fluorescent property. So, they may have potential for applications in heterogeneous catalysis and as contrast agents for bio-imaging and that work is underway in this laboratory. In order to get an in-depth idea of the origin of the UV–vis spectral properties of the ligands as well as of the complexes, DFT calculations have been performed whose results are significantly well matched with the experimental values.

Acknowledgements

The authors wish to thank the CSIR, New Delhi (01/(2464)/11/EMR-II dt 16-05-2011 to DD) for financial support. The generous help of Dr. Bijan Pal, Research Scholar, Department of Chemistry, University of Calcutta, India, for fluorescence study is also duly acknowledged.

Appendix A. Supplementary material

Supplementary data associated with this article can be found, in the online version, at <http://dx.doi.org/10.1016/j.molstruc.2013.03.051>.

References

- [1] S. De Feyter, F.C. De Schryver, Chem. Soc. Rev. 32 (2003) 139.
- [2] J.V. Barth, Annu. Rev. Phys. Chem. 58 (2007) 375.
- [3] J.A. Theobald, N.S. Oxtoby, M.A. Phillips, N.R. Champness, P.H. Beton, Nature 424 (2003) 1029.
- [4] Z. Li, B. Han, L.J. Wan, T. Wandlowski, Langmuir 21 (2005) 6915.
- [5] L.S. Pinheiro, M.L.A. Temperini, Surf. Sci. 601 (2007) 1836.
- [6] M.E. Canas-Ventura, Angew. Chem., Int. Ed. 46 (2007) 1814.
- [7] D. Payer, Chem. Eur. J. 13 (2007) 3900.
- [8] L. Kampschulte, S. Griessl, W.M. Heckl, M.J. Lackinger, Phys. Chem. B 109 (2005) 14074.
- [9] S. Furukawa, Angew. Chem., Int. Ed. 46 (2007) 2831.
- [10] E. Mena-Osteritz, P. Bäuerle, Adv. Mater. 18 (2006) 447.
- [11] A. Schenning, E.W. Meijer, Chem. Commun. (2005) 3245.
- [12] D.J. Diaz, S. Bernhard, G.D. Storrer, H.D. Abruna, J. Phys. Chem. B 105 (2001) 8746.
- [13] S. Stepanow, Nat. Mater. 3 (2004) 229.
- [14] J.-M. Lehn, Supramolecular Chemistry, VCH, Weinheim, 1995.
- [15] L.F. Lindoy, I.M. Atkinson, in: J.F. Stoddart (Ed.), Self-Assembly in Supramolecular Systems in Monographs in Supramolecular Chemistry, RSC, London, 2000.
- [16] M.C. Etter, Acc. Chem. Res. 23 (1990) 120.
- [17] G.R. Desiraju, Crystal Engineering, Elsevier, Amsterdam, 1998.
- [18] G.A. Jeffrey, W. Saenger, Hydrogen Bonding in Biological Structures, Springer, Berlin, 1991.
- [19] S. Subramanian, M.J. Zaworotko, Coord. Chem. Rev. 137 (1994) 357.
- [20] J.G. MacDonald, G.M. Whitesides, Chem. Rev. 94 (1994) 2383.
- [21] A. Ciesielski, C.-A. Palma, M. Bonini, P. Samori, Adv. Mater. 22 (2010) 3506.
- [22] (a) R. Melendez, A.D. Hamilton, Top. Curr. Chem. 198 (1998) 97; (b) C. Fu, F. Rosei, D.F. Perepichka, ACS Nano 9 (2012) 7973; (c) A. Cadeddu, A. Ciesielski, T.E. Malah, S. Hecht, P. Samori, Chem. Commun. 47 (2011) 10578; (d) A. Ciesielski, A. Cadeddu, C.-A. Palma, A. Gorczyński, V. Patroniak, M. Cecchini, Paolo Samori, Nanoscale 3 (2011) 4125.
- [23] (a) P.A. Tasker, P.G. Plioger, L.C. West, in: J.A. McCleverty, T.J. Meyer (Eds.), Comprehensive Coordination Chemistry II, vol. 9, Elsevier, 2004, p. 759.; (b) M. Wałęsa-Chorab, A. Gorczyński, M. Kubicki, Z. Hnatejko, V. Patroniak, Polyhedron 31 (2012) 51; (c) T. Chattopadhyay, M. Mukherjee, A. Mondal, P. Maiti, A. Banerjee, K.S. Banu, S. Bhattacharya, B. Roy, D.J. Chattopadhyay, T.K. Mondal, M. Nethaji, E.

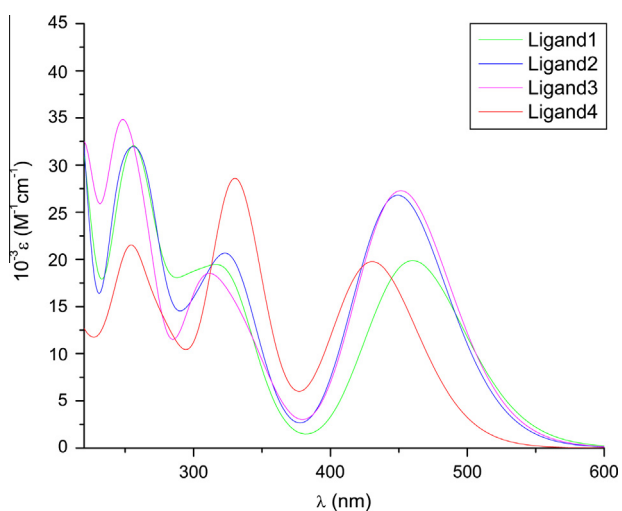


Fig. 4. Calculated absorption spectra of the ligands in DMSO.

- Zangrando, D. Das, *Inorg. Chem.* 49 (2010) 3121;
(d) T. Chattopadhyay, S. Islam, M. Nethaji, A. Majee, D. Das, *J. Mol. Catal. A: Chem.* 267 (2007) 255;
(e) T. Chattopadhyay, K.S. Banu, A. Banerjee, J. Ribas, A. Majee, M. Nethaji, D. Das, *J. Mol. Struct.* 833 (2007) 13.
- [24] P. Talukder, S. Shit, A. Sasmal, S.R. Batten, B. Moubaraki, K.S. Murray, S. Mitra, *Polyhedron* 30 (2011) 1767.
- [25] (a) D. Perrin, W. Armarego, *Purification of Laboratory Chemicals*, second ed., Pergamon Press, Oxford, 1981;
(b) J. Leonard, B. Lygo, J. Procter, *Praxis der Organischen Chemie*, Wiley-VCH, Weinheim, 1996.
- [26] H. Gottlieb, V. Kotlyar, A. Nudelman, *J. Org. Chem.* 62 (1997) 7512.
- [27] (a) A.D. Becke, *J. Chem. Phys.* 98 (1993) 5648;
(b) C. Lee, W. Yang, R.G. Parr, *Phys. Rev. B* 37 (1988) 785.
- [28] (a) P.J. Hay, W.R. Wadt, *J. Chem. Phys.* 82 (1985) 270;
(b) W.R. Wadt, P.J. Hay, *J. Chem. Phys.* 82 (1985) 284;
(c) P.J. Hay, W.R. Wadt, *J. Chem. Phys.* 82 (1985) 299.
- [29] Gaussian 03, Revision D.01, M.J. Frisch, G.W. Trucks, H.B. Schlegel, G.E. Robb, J.R. Cheeseman, J.A. Montgomery Jr., T. Vreven, K.N. Kudin, J.C. Burant, J.M. Millam, S.S. Iyengar, J. Tomasi, V. Barone, B. Mennucci, M. Cossi, G. Scalmani, N. Rega, G.A. Petersson, H. Nakatsuji, M. Hada, M. Ehara, K. Toyota, R. Fukuda, J. Hasegawa, M. Ishida, T. Nakajima, Y. Honda, O. Kitao, H. Nakai, M. Klene, X. Li, J.E. Knox, H.P. Hratchian, J.B. Cross, V. Bakken, C. Adamo, J. Jaramillo, R. Gomperts, R.E. Stratmann, O. Yazyev, A.J. Austin, R. Cammi, C. Pomelli, J.W. Ochterski, P.Y. Ayala, K. Morokuma, G.A. Voth, P. Salvador, J.J. Dannenberg, V.G. Zakrzewski, S. Dapprich, A.D. Daniels, M.C. Strain, O. Farkas, D.K. Malick, A.D. Rabuck, K. Raghavachari, J.B. Foresman, J.V. Ortiz, Q. Cui, A.G. Baboul, S. Clifford, J. Cioslowski, B.B. Stefanov, G. Liu, A. Liashenko, P. Piskorz, I. Komaromi, R.L. Martin, D.J. Fox, T. Keith, M.A. Al-Laham, C.Y. Peng, A. Nanayakkara, M. Challacombe, P.M.W. Gill, B. Johnson, W. Chen, M.W. Wong, C. Gonzalez, J.A. Pople, Gaussian, Inc., Wallingford, CT, 2004.
- [30] (a) R. Bauernschmitt, R. Ahlrichs, *Chem. Phys. Lett.* 256 (1996) 454;
(b) R.E. Stratmann, G.E. Scuseria, M.J. Frisch, *J. Chem. Phys.* 109 (1998) 8218;
(c) M.E. Casida, C. Jamorski, K.C. Casida, D.R. Salahub, *J. Chem. Phys.* 108 (1998) 4439.
- [31] (a) V. Barone, M. Cossi, *J. Phys. Chem. A* 102 (1998) 1995;
(b) M. Cossi, V. Barone, *J. Chem. Phys.* 115 (2001) 4708;
(c) M. Cossi, N. Rega, G. Scalmani, V. Barone, *J. Comput. Chem.* 24 (2003) 669.
- [32] L. Sun, L.J. Kepley, R.M. Crooks, *Langmuir* 8 (1992) 2101.
- [33] J. Dong, Y. Ozaki, K. Nakashima, *Macromolecules* 30 (1997) 1111.
- [34] M. Kogiso, T. Hanada, K. Yase, T. Shimizu, *Chem. Commun.* (1998) 1791.
- [35] M. Kogiso, Y. Okada, T. Hanada, K. Yase, T. Shimizu, *Biochim. Biophys. Acta, Gen. Subj.* 1475 (2000) 346.
- [36] M. Kogiso, Y. Okada, K. Yase, T. Shimizu, *J. Colloid Interface Sci.* 273 (2004) 394.
- [37] T.F. Jiao, J. Zhou, J.X. Zhou, L.H. Gao, Y.Y. Xing, X.H. Li, *Iran. Polym. J.* 20 (2011) 123.
- [38] N. Lomadze, H.J. Schneider, *Tetrahedron* 61 (2005) 8694.
- [39] W. Turbeville, P.K. Dutta, *J. Phys. Chem.* 94 (1990) 4060.
- [40] A. Mandal, A. Koll, A. Filarowski, D. Majumder, S. Mukherjee, *Spectrochim. Acta, Part A* 55 (1999) 2861.
- [41] A. Koll, A. Filarowski, D. Fitzmaurice, E. Waghorne, A. Mandal, S. Mukherjee, *Spectrochim. Acta, Part A: Mol. Biomol. Spectrosc.* 58 (2002) 197.